INTER-BAND COHERENCE OF SPLITTED WIDE BAND SAR IMAGES: A POTENTIALLY NEW INFORMATION CHANNEL

Dominique Derauw[1,2], Anne Orban[1] and Christian Barbier[1]

1. Centre Spatial de Liège, Space Environment and Remote Sensing Group, Angleur - Liège, Belgium; {dderauw / aorban / cbarbier}(at)ulg.ac.be
2. Royal Military Academy, Signal and Image Centre, Brussels, Belgium; dderauw(at)elec.rma.ac.be

ABSTRACT

Recently launched SAR sensors like TerraSAR-X or CosmoSkyMed are equipped with wide bandwidth radar signal emitters. Working at large bandwidth makes it possible to reach a metric range resolution which, combined with a spotlight mode, leads to Very High Resolution (VHR) SAR imagery.

One can also take advantage of this wide band to split it into sub-bands and generate several lower resolution images from the same master one, each centred on a slightly different central frequency.

These sub-images can then be used in a classical interferometric process to estimate the inter-band coherence of a given scene. This inter-band coherence reveals scatterers keeping a stable phase behaviour along with frequency shift. In this paper, a simple model derived from Zebker's model for randomly distributed surface scatterers is proposed and examples are presented showing that scatterers can have a behaviour that deviates from the model, leading to a new information channel.

INTRODUCTION

Most recently-launched spaceborne SAR sensors make use of wide bandwidth signals in order to reach a metric range resolution, while a metric azimuth resolution can be achieved through a spotlight acquisition mode. As an example, with a 150-MHz bandwidth, TerraSAR-X uses a radar signal bandwidth 10 times higher than ENVISAT ASAR, allowing it to potentially reach a 10 times higher resolution.

Wide band signals also provide a supplementary degree of freedom that is expected to be useful for absolute ranging (1). The principle was already proposed by Madsen and Zebker (2) using two sub-band interferograms as a possible solution for absolute phase unwrapping. The principle can be extended, segmenting the full wide band into sub-bands and generating several lower range resolution sub-images, each centred on a different frequency. Generating this *chromatic view* for each image of an interferometric pair makes it possible to generate as many interferograms as wanted, each having a different carrier frequency.

Scatterers keeping a coherent behaviour in each sub-band interferogram show a phase that varies linearly with the central frequency, the slope being proportional to the absolute optical path difference. This potentially solves the problem of phase unwrapping on a pixel by pixel basis (3,4).

The frequency-coherent scatterers are defined operationally as those pixels where the phases in the multi-frequency interferograms show a linear behaviour. In analogy with the temporal Persistent Scatterers (5), coherence thresholds can be used to define reliable scatterers (6) for split band interferometric processing.

In this paper, an innovative aspect aiming at analysing the information content within a single wide-band SAR acquisition is addressed at.

Sub-band splitting of a single wide band acquisition will give a chromatic view of the scene, each sub-band being centred on a different carrier frequency, and each observing the same on-ground scatterer distribution. One can thus measure the decorrelation between pairs of chromatic views through a classical interferometric process.

First, a simple coherence model derived from the Zebker model (7) is discussed, showing that, for randomly distributed surface scatterers, the coherence should fall to zero for non-overlapping sub-bands.

Second, we present an example using a TerraSAR-X acquisition, showing that inter-band coherence may deviate from this simple model. This is a consequence of the fact that observed scatterer distributions may differ locally from the underlying hypothesis of the model (i.e. randomly distributed surface scatterers). As a consequence, inter-band coherence bears information related to the scatterer distribution and to the scattering process within the resolution cell.

ADAPTED COHERENCE MODEL

Considering classical SAR interferometry in a monostatic configuration, two signals s_1 and s_2 are acquired by a single antenna observing the same area in two successive passes. If x and y are respectively the azimuth and ground range coordinates, the measured signals in the final processed images, at the position (x_0,y_0), are expressed by (7):

$$s_1 = \iint f(x-x_0, y-y_0)\, \mathrm{e}^{-\mathrm{j}\frac{4\pi}{\lambda}(r+y\sin\theta_1)} W(x,y)\,\mathrm{d}x\,\mathrm{d}y + n_1$$

$$s_2 = \iint f(x-x_0, y-y_0)\, \mathrm{e}^{-\mathrm{j}\frac{4\pi}{\lambda}(r+y\sin\theta_2)} W(x,y)\,\mathrm{d}x\,\mathrm{d}y + n_2$$

where r is the slant range to the considered point at position (x_0,y_0), $f(x,y)$ represents the complex backscatter function of each point of the surface, and $W(x,y)$ is the point target response of the acquisition system. n_i is the noise associated with each receiver. The angles θ_1 and θ_2 are the local incidence angles of the radar signals as depicted in Figure 1.

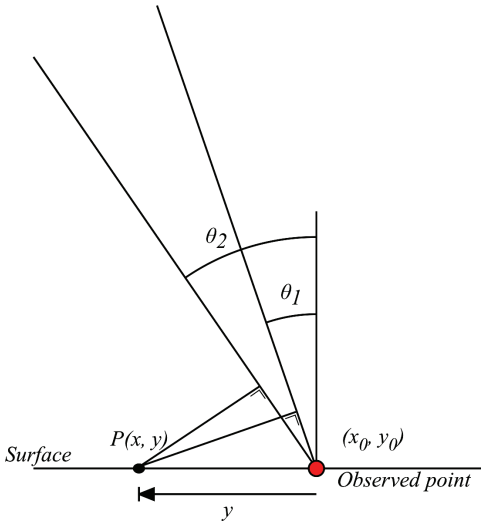

Figure 1: Schematic interferometric SAR viewing geometry.

The interferometric process is described through the cross-correlation of the two signals s_1 and s_2, i.e., $< s_1\, s_2^* >$.

In the Zebker model, it is assumed that one deals with uniformly distributed and uncorrelated surface scattering centres. Considering in addition a classical sinc impulse response, this cross-correlation is readily obtained. Evaluation of the cross-correlation followed by normalisation leads to the well-known expression for the geometrical decorrelation function (7):

$$\gamma = 1 - 2R_y\left(\frac{\sin\theta_1}{\lambda} - \frac{\sin\theta_2}{\lambda}\right) \cong 1 - \frac{2\cos\theta\,|\delta\theta|\,R_y}{\lambda}$$

where R_y is the ground range resolution of the system, θ is the average incidence angle and $\delta\theta = \theta_1 - \theta_2$.

The latter equation makes it possible to determine the critical baseline inducing complete geometrical decorrelation in the presence of randomly distributed surface scatterers.

Now, adapting the model to sub-band interferometry, one considers a single viewing angle θ, but two wavelengths λ_1 and λ_2. Therefore, the inter-band coherence becomes:

$$\gamma = 1 - 2R_y \sin\theta \left(\frac{1}{\lambda_1} - \frac{1}{\lambda_2} \right)$$

This expression for inter-band coherence may be expressed in terms of the central frequency separation of sub-bands using the relation expressing the ground range resolution with respect to the signal bandwidth *B*:

$$R_y \sin\theta = \delta r = c/2B$$

where *c* is the speed of light and δr is the slant range resolution. After a few calculations, one finds:

$$\gamma = 1 - \frac{\Delta\nu}{B}$$

where $\Delta\nu$ is the central frequency separation of sub-bands.

Similar to the critical baseline leading to full coherence loss in classical InSAR, the inter-band coherence is completely lost when the sub-band separation $\Delta\nu$ equals their bandwidth *B*.

DATA SET DESCRIPTION AND CLASSICAL INTERFEROMETRIC MEASUREMENTS

We used a TerraSAR-X spotlight interferometric pair downloaded from the InfoTerra web site. This data set is made of two Single Look Complex images acquired over Bergen, Norway, on November 24 and December 5, 2007. The available bandwidth is 150 MHz.

First, a classical interferometric process was performed to derive the interferometric coherence on the whole scene. The interferometric coherence along with the corresponding histogram and an amplitude image of the whole scene is represented in Figure 2.

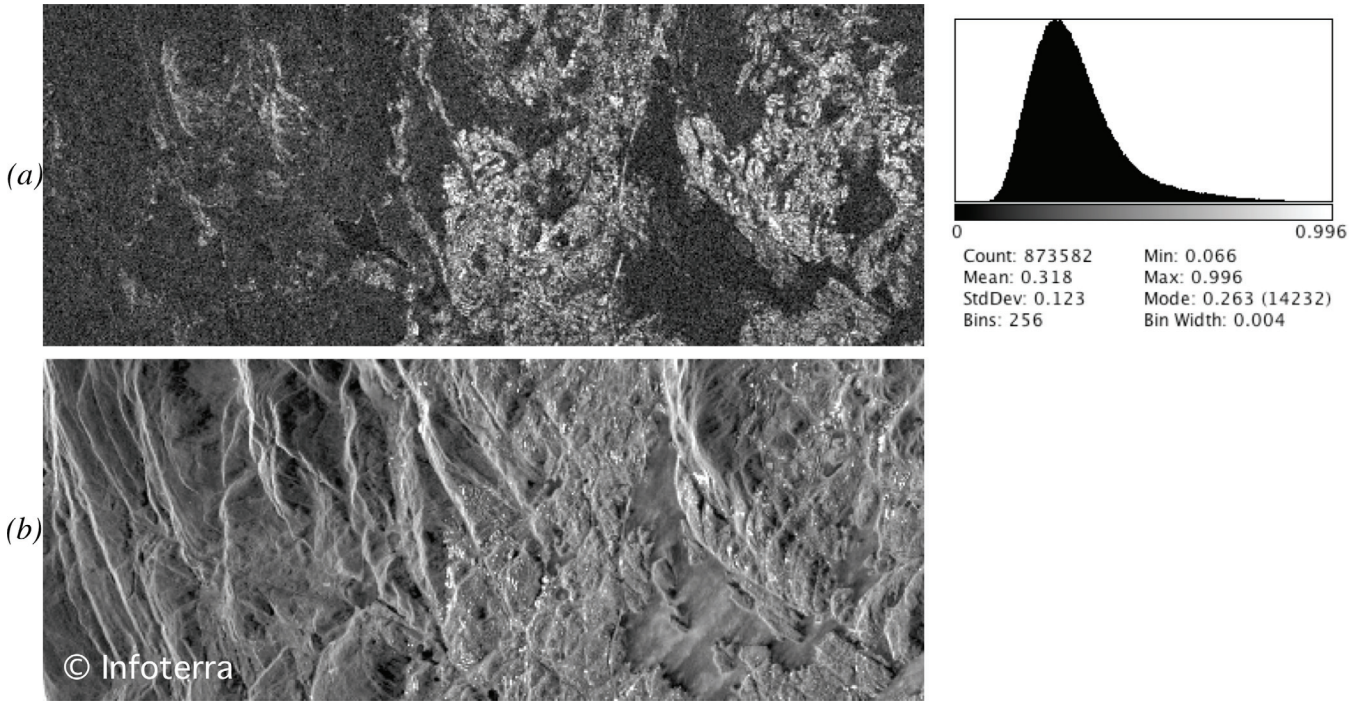

Figure 2: (a): Interferometric coherence and corresponding histogram. (b): Amplitude image of the observed scene.

SUB-BAND SPLITTING AND INTER-BAND COHERENCE MEASUREMENTS

After having computed the interferometric coherence, we performed a sub-band splitting of the master image of the interferometric pair to generate seven lower resolution sub-images.

The image chosen was first Fourier transformed along range. Then, the data was filtered with a moving filter in order to select the seven sub-bands. The chosen sub-band bandwidth B is 40MHz. The central frequencies of sub-bands are spaced every $\Delta\nu$ = 18.88 MHz to cover the full 150 MHz available bandwidth. Therefore, each sub-band overlaps its immediate neighbours by about 53%. The overlap between sub-bands $2\Delta\nu$ apart is about 5%. For higher sub-band separation no overlap occurs.

After sub-band filtering, each sub-band data is inverse Fourier transform to get back into the image domain, leading to seven sub-views, each centred on a slightly different carrier frequency. Considering two given sub-views as an interferometric pair makes it possible to estimate the underlying inter-band coherence.

These seven sub-views make it possible to generate 21 potential interferometric pairs. Whatever sub-view considered as master image, the results appear to be the same: the coherence remains partially preserved when performing interferometry with the sub-views obtained from the sub-band immediately before or after the reference one. Then, the coherence rapidly decreases with a gap in central frequencies but some areas keep a high level of coherence even if there is no overlap between sub-bands.

Figure 3 shows the 6 inter-band coherence images obtained when considering the sub-view centred on the full-resolution carrier frequency as master. The sub-view central frequency of the slaves increases from bottom to top of the figure. Corresponding histograms are shown on the left of each coherence image.

Figures 3d and c are obtained considering slave sub-views just before and just after the master one in terms of sub-band central frequencies. For those sub-views, spectra overlap partially by about 53%. As can be seen, average values of the histograms are very close to that value. It is thus in good agreement with the adapted Zebker model.

When the sub-band overlap is of only a few percent, the coherence still decreases but not to the expected level. Some clearly scene-related structures appear, some points showing quite a high coherence level. Even if there is no overlap between sub-bands, the coherence does not fall to zero as expected from the theoretical model. The same structures stay still well observable. When no overlapping occurs, the inter-band coherence appears roughly similar to the interferometric coherence shown in Figure 2.

The fact that the coherence does not fall to zero with sub-band separation as expected from the model may have several reasons:

1. Coherence is not measured but estimated and it is well known that coherence estimators are biased. The estimation is only correct for a coherence of 1. This bias is clearly visible on coherence histograms; the minimum value never falls below 4%.
2. The model is valid only for random surface scatterers. The observed surface cannot be considered as purely made of random surface scatterers. There are forested areas in which volume scattering dominates and also urban areas in which a dihedral scattering process dominates. Moreover, the scene considered is a spotlight scene with a very high spatial resolution. In such a metric resolution cell, distribution randomness of scatterers with respect to the wavelength is less granted than with classical resolution sensors like ERS or ENVISAT offering a resolution cell having an area 100 times larger. At a very high resolution chances are rising that a single scatterer dominates the background, invalidating the basis hypothesis of the model. The same is observed and used in permanent or persistent scatterer interferometry techniques.

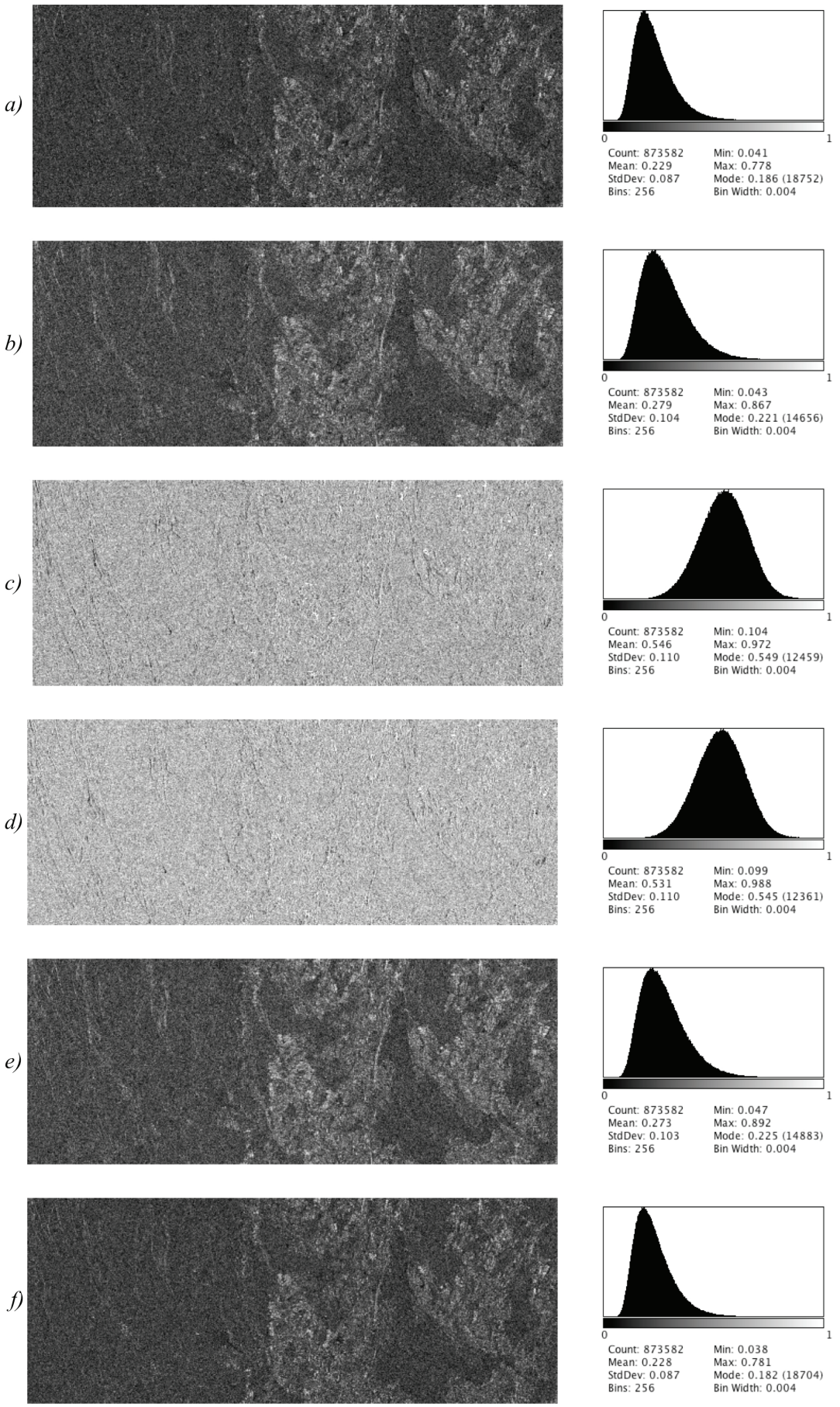

Figure 3: Inter-band coherence measurements with corresponding histograms.

The fact that the model fails to describe a real scene is interesting in the sense that deviation with respect to random surface scattering reveals other scatterer distributions and scattering processes. Consequently, inter-band coherence, like interferometric coherence, can be considered as an information channel related to local scatterer distributions and scattering processes; this information channel being extracted from a single acquisition.

Considering a possible deviation with respect to the main hypothesis, i.e. a random distribution of surface scatterers, inter-band coherence should make it possible to discriminate volume or dihedral scattering processes from surface scattering. Tests are currently being performed to analyse the ability to use inter-band coherence in marine surveillance, for example, using the coherence level to discriminate vessels from the surrounding sea in a single wide-band SAR acquisition.

CONCLUSIONS

The information content of a wide band SAR acquisition through sub-band splitting and inter-band coherence measurements was studied. The Zebker model proposed for classical InSAR was adapted to describe inter-band coherence. With respect to this simple model, the coherence should stay proportional to sub-band overlap. Discrepancies with respect to this simple model were observed splitting a TerraSAR-X spotlight acquisition into seven sub-views and performing inter-band coherence measurements. The coherence decreases, but does not fall to zero as expected. Like in interferometric coherence, inter-band coherence reveals scene related features. Obviously, one of the key assumption of the model, i.e. random distribution of surface scatterers, failed to describe fully the scene behaviour. Inter-band coherence can thus be considered as an information channel related to local scatterer distributions and scattering processes; this information channel being extracted from a single wide-band SAR acquisition.

ACKNOWLEDGEMENTS

This work was carried out under ESA contract No 21319/07/NL/HE.

REFERENCES

1 Bamler R & M Eineder, 2004. Split band interferometry versus absolute ranging with wideband SAR systems. In: Proceedings of the International Geoscience & Remote Sensing Symposium (IGARSS'04), Vol. II, 980-984

2 Madsen S N & H A Zebker, 1992. Automated absolute phase retrieval in across-track interferometry. In: Proceedings of the International Geoscience & Remote Sensing Symposium (IGARSS'92), Vol. II, 1582-1584

3 Veneziani N, F Bovenga & A Refice, 2003. A wide-band approach to absolute phase retrieval in SAR interferometry. Multidimensional Systems and Signal Processing, 14: 183-205

4 Bamler R & M Eineder, 2005. Accuracy of differential shift estimation by correlation and split-bandwidth interferometry for wideband and delta-k SAR systems. IEEE Geoscience and Remote Sensing Letters, 2(2): 151-155

5 Ferretti A, C Prati & F Rocca, 2001. Permanent scatterers in SAR interferometry. IEEE Transactions in Geosciences and Remote Sensing, 39(1): 8-20

6 Veneziani N & V M Giacovazzo, 2006. A multi-chromatic approach to SAR interferometry. Differential analysis of interferograms at close frequencies in the spatial domain and frequency domain. In: Proceedings of the International Geoscience & Remote Sensing Symposium (IGARSS'06) 3706-3709

7 Zebker H A & J Villasenor, 1992. Decorrelation in interferometric radar echoes. IEEE Transactions in Geosciences and Remote Sensing, 30(5): 950-959